

IL-22 Alleviates Sepsis-Induced Acute Lung Injury by Inhibiting Epithelial Cell Apoptosis Associated with STAT3 Signalling

Chiying Zhu^{1,2,*}, Jiabo Chen^{2,3,*}, Zhengzheng Yan⁴, Fei Wang⁵, Ziqi Sun^{2,3}, Zeyu Liu^{1,2}, Ying Li⁴, Xiaona Chen^{2,6}, Ziwei Bao¹, Quan Li^{1-3,6}, Zhixia Chen^{2,3}

¹Shenzhen Clinical Medical College, Guangzhou University of Chinese Medicine, Shenzhen, 518116, People's Republic of China; ²Department of Anesthesiology, National Cancer Center/National Clinical Research Center for Cancer/Cancer Hospital & Shenzhen Hospital, Chinese Academy of Medical Sciences and Peking Union Medical College, Shenzhen, 518116, People's Republic of China; ³Department of Anesthesiology, School of Medicine, The First Affiliated Hospital of Nanchang University, Nanchang University, Nanchang, 330006, People's Republic of China; ⁴Laboratory Animal Research Center, The Tenth Affiliated Hospital, Southern Medical University (Dongguan People's Hospital), Dongguan, 523000, People's Republic of China; ⁵The Tenth Affiliated Hospital, Southern Medical University (Dongguan People's Hospital), Dongguan, 523059, People's Republic of China; ⁶Department of Biology, School of Medicine, Southern University of Science and Technology, Shenzhen, 518055, People's Republic of China

*These authors contributed equally to this work

Correspondence: Zhixia Chen; Quan Li, Department of Anesthesiology, National Cancer Center/National Clinical Research Center for Cancer/Cancer Hospital & Shenzhen Hospital, Chinese Academy of Medical Sciences and Peking Union Medical College, Shenzhen, 518116, People's Republic of China, Email Chenzhixia2007@126.com; quanligene@126.com

Purpose: Sepsis is a critical condition characterized by organ dysfunction due to an aberrant response to infection, which results in a life-threatening situation. The lung, which is the most vulnerable target organ, is often severely damaged during sepsis. Research has demonstrated that interleukin-22 (IL-22), which is secreted by various immunocytes, can mitigate inflammation-associated diseases. Nevertheless, the precise function of IL-22 in sepsis-induced acute lung injury (SALI) is still unclear. This study aimed to investigate the therapeutic efficacy of IL-22 in sepsis and explore the regulatory mechanisms involved.

Methods: A mouse caecal ligation and puncture (CLP) model of sepsis was established, and the effect of IL-22 was investigated as indicated. Immunohistochemistry, qRT-PCR, ELISA, immunofluorescence, TUNEL, Western blotting, and flow cytometry assays were applied to investigate the protective efficacy and involved pathways. Additionally, an in vitro model of lipopolysaccharide (LPS)-induced bronchial epithelial cell (BEAS-2B) apoptosis was established, and these cells were treated with or without recombinant IL-22 (rIL-22) to further evaluate the effect of IL-22 and the underlying mechanism.

Results: The experimental results clearly confirmed that the levels of IL-22 were increased in the serum and lung tissue after CLP. The administration of rIL-22 was observed to increase the survival rate of septic mice. Notably, rIL-22 treatment resulted in decreased levels of proteins and a decreased cell number in the bronchoalveolar lavage fluid, as well as in a reduction in inflammatory cytokine release into the serum. Importantly, rIL-22 mitigated SALI by inhibiting lung cell apoptosis in septic mice. Furthermore, the results revealed that rIL-22 attenuated apoptosis of lung epithelial cells via the activation of the STAT3 signalling pathway.

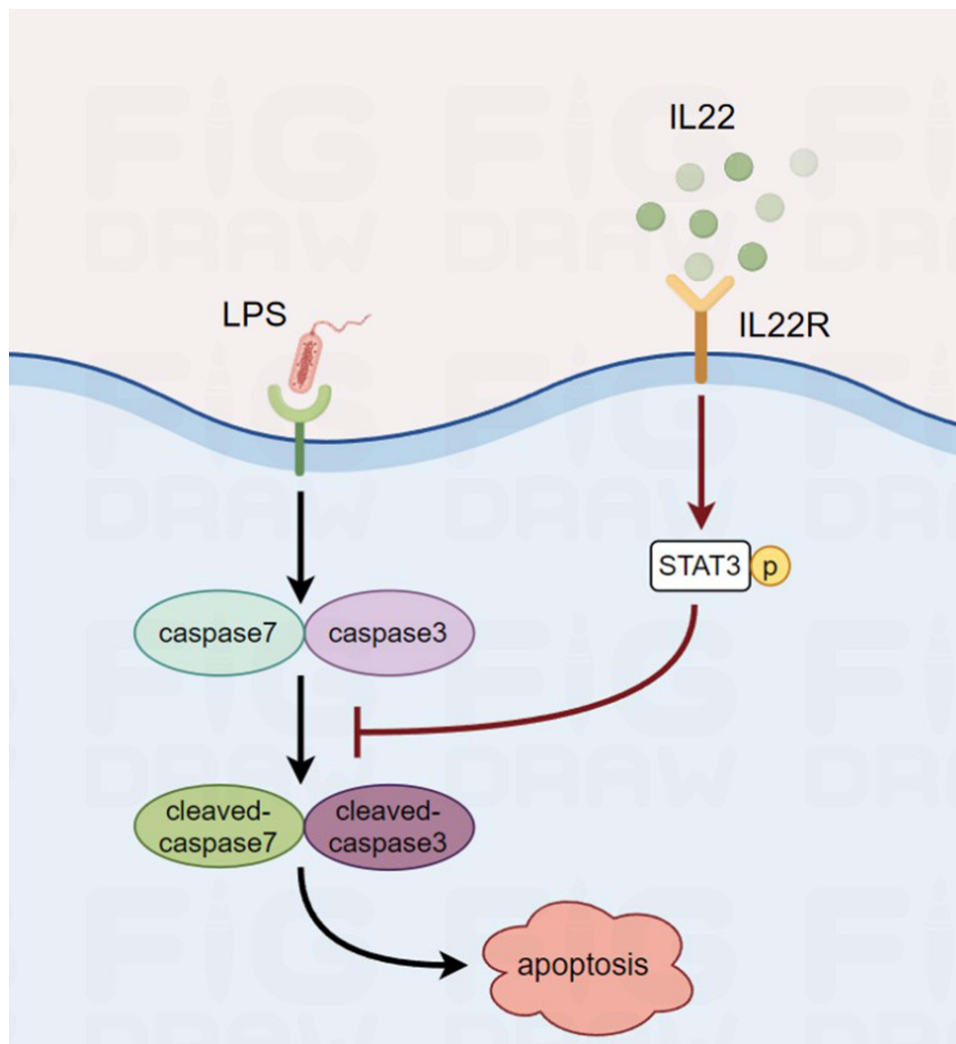
Conclusion: The results of this study suggest that IL-22 alleviates lung epithelial cell apoptosis to protect mice against SALI in association with the STAT3 signalling pathway, highlighting the potential therapeutic value of IL-22 against sepsis.

Keywords: IL-22, sepsis, acute lung injury, apoptosis, STAT3

Introduction

Sepsis, which is associated with high morbidity and mortality rates, is a critical condition that is characterized by life-threatening organ dysfunction due to an aberrant host response to infection. The lung is the most vulnerable target organ in the progression of sepsis.¹ Although great efforts have been made worldwide, there are still no effective strategies for treating acute lung injury (ALI) in the clinic. ALI is a prevalent inflammatory lung disorder that is characterized by

Graphical Abstract



excessive generation of proinflammatory mediators and the infiltration of inflammatory cells.^{2,3} Emerging evidence indicates that alveolar epithelial cell apoptosis is closely associated with the pathogenesis of ALI.⁴

IL-22, a member of the IL-10 cytokine family, is secreted by a variety of immune cells, including CD4⁺ T cells, CD8⁺ T cells and T-helper 17 (Th17) cells, during bacterial infection.^{5–7} IL-22 binds tightly to the IL-22 receptor (IL-22R), which is expressed specifically on the surface of epithelial cells in the bronchi, liver, pancreas, and intestine.⁸ Therefore, IL-22 plays a crucial role in mediating communication between immune cells and parenchymal cells (especially epithelial cells). IL-22 binds to the IL-22R complex and triggers downstream signalling pathways, including the signal transducer and activator of transcription 1/3/5 (STAT1/3/5), mitogen-activated protein kinase (MAPK) and nuclear factor kappa-B (NF-κB) pathways, subsequently exerting immunoregulatory effects.^{9–11}

Numerous studies have demonstrated protective properties of IL-22 in different lung injury models, such as viral infection,¹² angiotensin II-induced acute lung injury and ventilator-induced lung injury^{13,14} models. The mechanisms of the protective effect of IL-22 were revealed to involve the suppression of bacterial growth and the inhibition of hepatocyte autophagy via the ATF4/ATG7 signalling pathway.^{15,16} In orally infected IL-22R^{-/-} mice, the intestinal damage and bacterial translocation were markedly increased.¹⁷

The levels of IL-22 are notably greater in the serum of patients with acute respiratory distress syndrome (ARDS) than in healthy individuals,¹⁸ while the concentrations of IL-22 in the bronchoalveolar lavage fluid (BALF) are significantly reduced in patients with ARDS.¹⁹ However, another study indicated that inhibiting IL-22 by IL-22-binding protein (IL-22BP) led to increased bacterial clearance in the liver and kidney and reduced kidney injury, which was revealed by a decrease in the serum creatinine level in colon ascendens stent peritonitis-induced sepsis.²⁰ Therefore, the effects of IL-22 may vary in different organs or under different disease conditions. Although several studies have investigated the role of IL-22 in modulating inflammatory diseases, its role in SALI has not been fully elucidated. In the present study, we found notable increases in the levels of IL-22 in the serum and lung tissue of mice subjected to CLP. rIL-22 treatment alleviated SALI by reducing lung epithelial cell apoptosis, which was correlated with STAT3 activation.

Materials and Methods

Mice

Specific pathogen-free male C57BL/6 mice (8 weeks, weighing approximately 22 g) were purchased from Guangzhou Jinwei Biotechnology Co., Ltd. The mice were housed in the Experimental Animal Centre of the Tenth Affiliated Hospital of Southern Medical University in an air-conditioned environment at $24 \pm 1^\circ\text{C}$. The mice had unrestricted access to water and food. The Ethics Committee of the Tenth Affiliated Hospital of Southern Medical University approved all the procedures related to the care and use of mice following the Guide for the Care and Use of Laboratory Animals, Eighth Edition (IACUC-AWEC-202403113).

CLP

We used 8–12-week-old mice for the experiments. After inducing anaesthesia with sevoflurane, the peritoneal cavity was incised. The caecum was exteriorized and tied at different locations (distal to the ileocecal valve) with a 7–0 suture. Following the closure of the abdominal wall, each mouse was subcutaneously injected with 1 mL of sterile saline for fluid resuscitation. The procedure aimed to induce mid-grade sepsis by ligating 50% of the caecum, whereas high-grade sepsis was induced by ligating 75% of the caecum.²¹ The control animals underwent a similar procedure but without caecal perforation. The mice received an injection of rIL-22 (R&D, 782-IL-010) at 250 $\mu\text{g/kg}$ either one hour before or one hour after CLP through the tail vein. For experiments involving the neutralization of IL-22, the mice were treated with 100 μg of functional-grade anti-IL-22 monoclonal antibody by intraperitoneal injection (Thermo Fisher Scientific, 16–7222-85).²² The survival status of the mice was observed at intervals of 6 hours following CLP surgery, and the time of natural death within 72 hours of the initiation of CLP was documented.

Cell Culture

BEAS-2B cells were obtained from Zhejiang Meisen Cell Technology Co., Ltd. The cells were cultured with high-glucose DMEM supplemented with 10% foetal bovine serum and 100 U/mL penicillin–streptomycin. The cells were grown at 37°C in an incubator with 5% CO_2 and appropriate humidity.

Total Protein Analysis in BALF

Total protein samples were collected 12 hours after the animal model was established. The neck skin of each mouse was incised in the middle, and the muscles and fascia surrounding the trachea were bluntly separated to expose the trachea. The upper end of the trachea was incubated, and the lung was subjected to three consecutive rinses with 0.8 mL of PBS each. The BALF was obtained and centrifuged at 4°C and $3000 \times g$ for 10 minutes. The supernatant was collected for protein content assessment via the BCA method.

Cell Counts in BALF

BALF was collected as described above. The collected cells were resuspended in 100 μL of PBS, and 25 μL was removed for counting.

Lung Wet-to-Dry Weight Ratio

The mice were humanely euthanized via carbon dioxide (CO₂) overdose 12 hours after the animal model was established, and the lungs were removed by severing the trachea. The wet weight of the lung was measured. The lungs were then transferred to an incubator and subjected to drying at 60°C for 72 h. The dry weight of the lungs was measured, and the W/D weight ratio of the lungs was calculated.

Histopathology and Biochemistry Analysis

Lung tissue was collected and preserved in 4% PFA. After dehydration and paraffin embedding, the tissue sections were stained to examine histopathological alterations. The histological quantitative scoring criteria included the following: 1) pulmonary tissue and interstitial oedema, 2) bleeding and red blood cell exudation, 3) aggregation of inflammatory cells, and 4) increased alveolar wall thickness.²³ The criteria were assessed via a scoring system ranging from 0 to 4, where 0 represents no damage, 1 indicates mild damage, 2 indicates moderate damage, 3 indicates severe damage, and 4 indicates very severe damage. This scoring system was used to calculate the lung tissue injury score.

Immunohistochemistry

Sections of the paraffin-embedded lung tissue were subjected to dewaxing and hydration. Citrate buffer was used for antigen retrieval. The areas to be stained were circled with an immunohistochemical pen and blocked. Next, the sections were incubated with primary and secondary antibodies and then tagged with horseradish peroxidase. Staining was performed via DAB working solution and haematoxylin counterstaining. The sections were dehydrated and mounted for observation.

Real-Time Quantitative PCR

Total RNA was extracted from lung tissues via the Eastep[®] Super Total RNA Extraction Kit (LS1040). The ReverTra Ace[®] qPCR RT Kit (FSQ-101) was used to generate cDNA. Real-time quantitative PCR was conducted with Hieff[®] qPCR SYBR Green Master Mix (11202ES50) on an ABI QuantStudio 5 Real-Time PCR System (Thermo Fisher Scientific, Waltham, USA). The 2- $\Delta\Delta$ Ct method was used to calculate gene expression, which was normalized to the expression of GAPDH. The primer sequences (mouse) used were as follows: IL-6 forwards: 5'-ATGAACCTCTTCTCCACAAGCGC-3'; reverse: 5'-GAAGAGCCCTCAGGCTGGACTG-3'; IL-1 β forwards: 5'-ATGGCAGAAGTACCTAAGCTCGC-3'; reverse: 5'-ACACAAATTGTCATGGTGAAGTCAGTT-3'; Tumour necrosis factor- α (TNF- α) forwards: 5'-ATGAGCACTGAAAGCATGATCCGG-3'; reverse: 5'-GCAATGATCCCAAAGTAGACCTGCCC-3'; IL-22 forwards: 5'-CCCTCAATCTGATAGGTCCA-3'; reverse: 5'-GCAGGTCATCACCTTGACA-3'; GAPDH forwards: 5'-ACCACAGTCCATGCCATCAC-3'; reverse: 5'-TCCACCACCCTGTTGCTGTA-3'.

Enzyme-Linked Immunosorbent Assay (ELISA)

The serum levels of inflammatory cytokines, including IL-1 β (Proteintech, KE10003), TNF- α (Proteintech, KE10002) and IL-6 (Proteintech, KE10007), were determined via ELISA kits according to the manufacturers' protocols.

Terminal Deoxynucleotidyl Transferase-Mediated Nick-End Labelling (TUNEL) Assay

To assess apoptosis in the lung tissue of the mice in each group, a TUNEL assay was conducted with a TUNEL Apoptosis Assay Kit (Beyotime, C1086) in accordance with the guidelines provided by the manufacturer. The stained sections were scanned, and TUNEL-positive cells exhibited red fluorescence. Three random fields were selected from each slide for analysis. The number of total cells and TUNEL-positive cells in each field were then identified using ImageJ, and the TUNEL-positive cell ratio was calculated using the following formula: TUNEL-positive cell number/total cell number \times 100%.

Western Blotting

Lung tissue and cells were disrupted by homogenization in cell lysis buffer (10X; 9803S, CST) containing protease and phosphatase inhibitors. A BCA protein assay was used to determine the protein concentration. The protein samples were

subsequently separated via SDS polyacrylamide gel electrophoresis and then transferred onto PVDF membranes. After being blocked with 1% BSA at room temperature for 1 hour, the membranes were incubated with primary antibodies specific for the target proteins overnight at 4°C. The antibodies against β -actin (#4970, 1:5000), caspase-3 (#9662, 1:1000), cleaved caspase-3 (#9661, 1:800), caspase-7 (#9492, 1:1000), cleaved caspase-7 (#9491, 1:1000), STAT3 (#9139, 1:1000) and p-STAT3 (#9145, 1:1000) were obtained from Cell Signalling Technology and diluted to the indicated ratio. After three washes with TBST, the membranes were incubated with diluted secondary antibodies at a ratio of 1:3000 at room temperature for 1 hour. The membranes were washed three times with TBST, then treated with an enhanced chemiluminescence (ECL) substrate, and visualized with a Tanon 5200 Multi chemiluminescent imaging system (Shanghai, China). All of the above consumables were obtained from Thermo Scientific.

Flow Cytometry

BEAS-2B cells were collected after the indicated treatments. The supernatant was carefully discarded. Then, 100 μ L of binding buffer was added, and the mixtures were mixed gently to form a single-cell suspension. The samples were stained with Annexin V-FITC and PI according to the instructions and then incubated for 10 minutes in a light-free environment. Next, 400 μ L of binding buffer was added, followed by thorough mixing of the samples. The samples were subsequently analysed via a flow cytometer. (Agilent Technologies, NovoCyte Quanteon, Santa Clara, USA).

Cell Viability and Lactate Dehydrogenase (LDH) Activity Assays

To investigate the effect of LPS on the apoptosis of lung epithelial cells, a total of 1×10^4 BEAS-2B cells were treated with various concentrations (0, 1, 10, 100, 200, and 500 μ g/mL) of LPS (L2630-100mg, Sigma-Aldrich) for 12 or 24 hours and then subjected to the CCK-8 assay (HY-K0301, MCE) and lactate dehydrogenase (LDH) activity assay (G1780, Promega). To explore the protective effect of IL-22 against apoptosis, cells were pretreated with various concentrations (0, 10, 50, 100, and 200 ng/mL) of rIL-22 for 24 hours and then treated with LPS (500 μ g/mL) for the indicated times, followed by the CCK-8 assay. All the experiments involving cell culture were conducted in triplicate. In addition, cells were pretreated with rIL-22 (50 ng/mL) for 24 hours and then stimulated with LPS (500 μ g/mL) for 24 hours for further study.

Immunofluorescence Imaging

The cells were plated in glass-bottomed confocal plates and stimulated with LPS (500 μ g/mL) for 24 hours with or without rIL-22 (50 ng/mL) pretreatment. The samples were subjected to a series of steps, including fixation, permeabilization, blocking and incubation with an anti-cleaved caspase-3 antibody (1:500) overnight at 4°C. After three washes with PBS, the cells were incubated with a diluted fluorescein-conjugated secondary antibody at a ratio of 1:1000 at room temperature for 1 hour. The cells were subjected to DAPI staining. A Zeiss confocal microscope (Zeiss LSM900, Oberkochen, Germany) was used for analysis and recording.

Statistical Analysis

The data obtained from three separate experiments are presented as the means \pm standard deviations. A two-tailed unpaired Student's *t* test was used for comparisons between two groups, and one-way analysis of variance (ANOVA) with Bonferroni's multiple comparisons test were used for comparisons among multiple groups. Statistical comparison of Kaplan–Meier survival curves was conducted via the log-rank (Mantel–Cox) test. Statistical analysis was performed, and graphs were generated via GraphPad Prism 8.0 software. *P* values <0.05, 0.01, and 0.001 were considered to indicate statistical significance.

Results

The Expression of IL-22 Was Increased in Septic Mice

The contribution of IL-22 to inflammatory diseases remains unclear.^{18,19} To determine the levels of IL-22 in mice with sepsis, we collected mouse serum at the indicated times after the CLP procedure. We observed that the serum IL-22 level was substantially elevated in a time-dependent manner (Figure 1A). To further determine whether IL-22 secretion is correlated with the severity of sepsis, we generated a CLP mouse model as described above.²¹ The level of IL-22 was

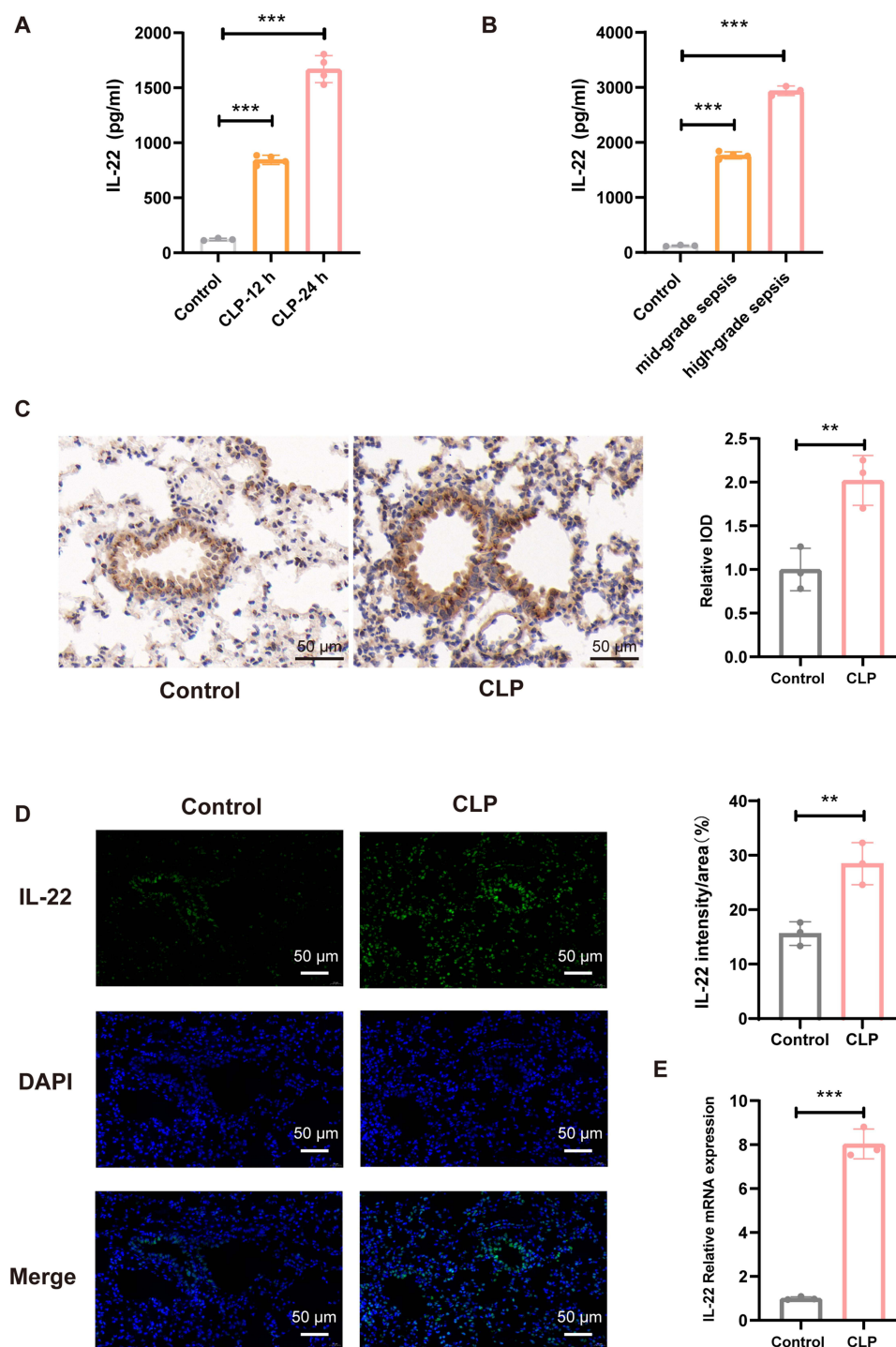


Figure 1 The expression of IL-22 was increased in the serum and lungs of septic mice. The mice were divided into a control group (Control) and a CLP group (CLP). Lung tissue was collected 12 hours after CLP at the indicated times ($n=3$). **(A)** Serum levels of IL-22 in mice at different time points after CLP. **(B)** Serum levels of IL-22 in mice subjected to different grades of CLP at 24 hours. **(C)** Immunohistochemical staining for IL-22 in lung sections. Reddish-brown staining indicates IL-22-positive cells. Scale bar, 50 μ m. **(D)** IL-22 in lung sections was stained for immunofluorescence imaging. Green signals are from immunostaining with an IL-22 antibody, and blue signals represent nuclei that are stained with DAPI. Scale bar, 50 μ m. **(E)** The mRNA level of IL-22 in lung tissue. Significant differences were determined by a two-tailed unpaired Student's *t*-test (**C–E**) or one-way ANOVA with Bonferroni's multiple comparisons test (**A and B**). ** $P<0.01$, *** $P<0.001$.

markedly greater in the mice subjected to high-grade CLP than in the mice subjected to mid-grade CLP (Figure 1B). The immunohistochemistry and immunofluorescence results similarly revealed that IL-22 expression was markedly increased at 12 hours in the lung tissue of sepsis mice. We observed that IL-22 was localized mainly to the bronchial epithelium, as

IL-22R is expressed specifically on the surface of epithelial cells⁸ (Figure 1C and D). Moreover, the mRNA level of IL-22 in murine lung tissue was significantly increased after CLP surgery (Figure 1E). These findings suggest that the level of IL-22 not only increases during sepsis but also positively correlates with the severity of sepsis.

rIL-22 Protected Mice Against SALI and the Inflammatory Response

After confirming the increase in IL-22 release during sepsis, we examined whether increasing IL-22 *in vivo* could mitigate sepsis progression. As shown in Figure 2A and B, compared with no treatment, rIL-22 administration 1 hour before or 1 hour after CLP clearly increased the survival rates of the mice. The lung is the most vulnerable target organ in sepsis progression.¹ To validate the effect of IL-22 on SALI in mice, rIL-22 was administered 1 hour before CLP surgery. The lung tissue was collected at 12 hours after CLP for further analysis. As shown in Figure 2C and D, histopathological examination revealed notable alleviation of lung tissue injury following the administration of rIL-22 compared with that in the CLP group. Furthermore, IL-22 significantly attenuated the CLP-induced increase in total cell counts and protein levels (Figure 2E and F). The lung W/D ratio was assessed as an indicator of pulmonary oedema.²⁴ There was a noteworthy increase in the lung W/D ratio after CLP. The administration of rIL-22 markedly reduced the W/D ratio (Figure 2G). In addition, compared with CLP alone, treatment with rIL-22 resulted in substantial decreases in the serum levels of IL-1 β , IL-6, and TNF- α (Figure 2H). Moreover, the administration of rIL-22 resulted in a significant reduction in the mRNA levels of IL-1 β , IL-6, and TNF- α in the lungs of the mice. (Figure 2I). These data suggest a beneficial role of IL-22 in SALI.

IL-22 nAb Exacerbated SALI and the Inflammatory Response During Sepsis

To further investigate the role of IL-22 in sepsis, we examined whether the inhibition of IL-22 exacerbates the progression of SALI. IL-22 nAb was administered 24 hours before mild-grade CLP surgery. As shown in Figure 3A and B, histopathological examination revealed more severe lung tissue damage after CLP surgery in the IL-22 nAb-treated group than in the untreated group. Additionally, neutralization of IL-22 further increased the cell counts and protein contents in the BALF of septic mice (Figure 3C and D). The administration of the IL-22 nAb also increased the W/D ratio (Figure 3E). The serum levels of inflammatory cytokines showed that IL-22 nAb treatment also promoted disease-associated increases in IL-6 and TNF- α (Figure 3F). These results revealed the protective properties of IL-22, highlighting its potential to alleviate the pathological processes associated with ALI *in vivo*.

rIL-22 Inhibited Apoptosis in SALI Mice

Apoptosis plays a deleterious role in the pathophysiology of SALI.⁴ To determine whether IL-22 inhibits apoptosis in mice with SALI, we quantified the rate of apoptosis in the lungs of CLP mice after rIL-22 treatment via TUNEL staining. As expected, the number of TUNEL-positive cells in the CLP group was significantly greater than that in the control group, whereas the number of TUNEL-positive cells induced by CLP was notably lower after rIL-22 treatment (Figure 4A). Previous research has indicated that caspase-3 and caspase-7 are important indicators of the occurrence of apoptosis.²⁵ We collected mouse lung tissue and examined the expression of relevant proteins via Western blotting. Compared with that in the control group, the expression of caspase-3 /7 did not increase, but a notable increase in the level of cleaved caspase-3/7 was observed in the CLP group. Treatment with rIL-22 considerably inhibited the upregulation of cleaved caspase-3/7 expression induced by CLP (Figure 4B). Furthermore, the cleaved caspase-3 level significantly increased in the lung epithelial cells after CLP modelling (Supplementary Figure 1). In contrast, pretreatment with the IL-22 nAb increased the number of TUNEL-positive cells in the lung (Supplementary Figure 2). Collectively, these data suggest that IL-22 plays a protective role by suppressing apoptosis in the pulmonary tissues of septic mice.

rIL-22 Inhibited Apoptosis in LPS-Stimulated Lung Epithelial Cells

To confirm the role of IL-22 in sepsis progression and determine the underlying mechanism, we used LPS-stimulated BEAS-2B cells to simulate the inflammatory conditions observed during sepsis. To determine the optimal concentration of LPS that affects BEAS-2B cell viability and LDH activity, we stimulated BEAS-2B cells with different concentrations of LPS for 12 and 24 hours. As shown in Figure 5A and B, stimulating BEAS-2B cells with 500 μ g/mL LPS attenuated

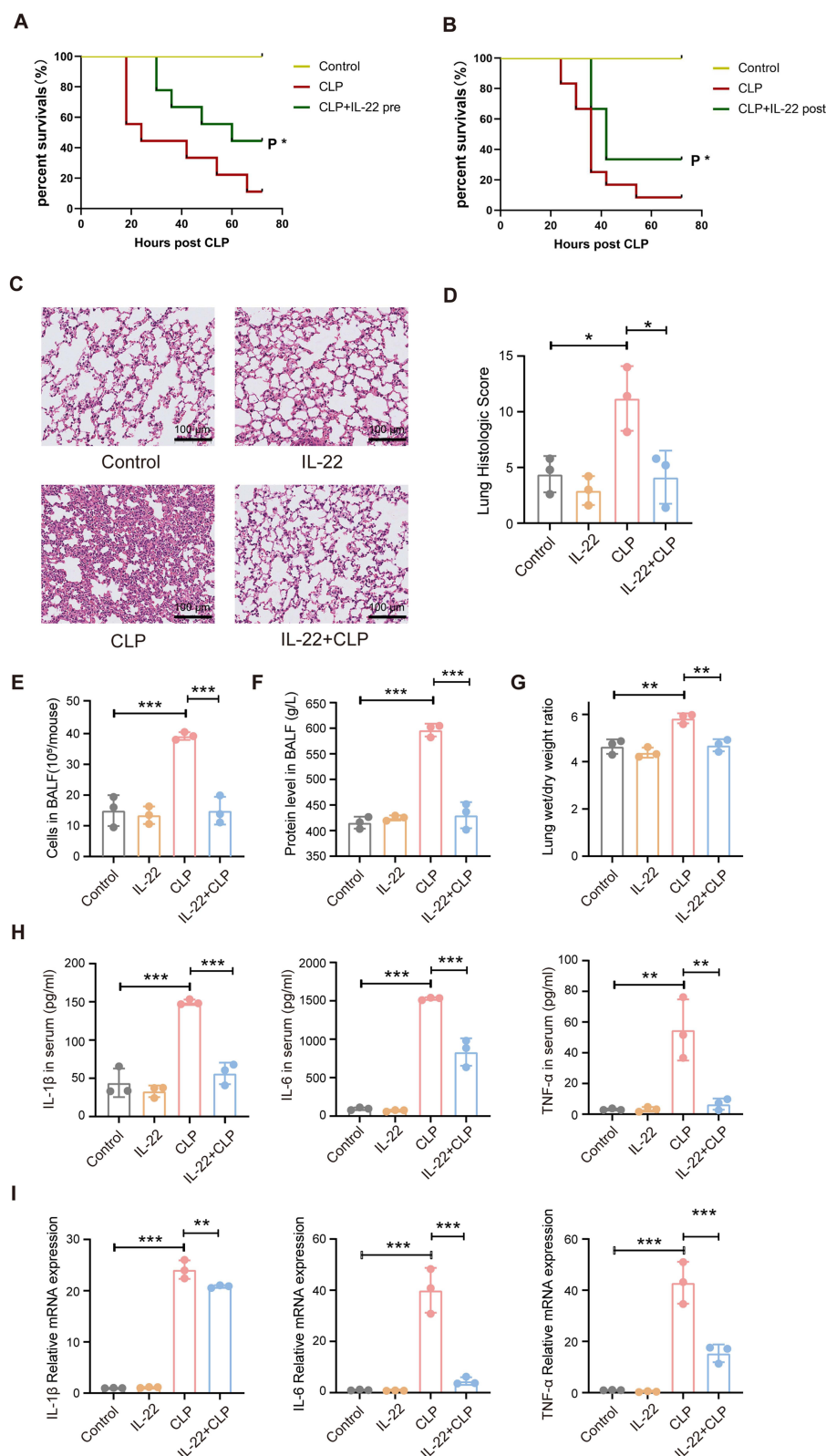


Figure 2 rIL-22 protects mice against SALI. **(A)** Survival of mice injected with rIL-22 or vehicle 1 hour before CLP surgery (n = 12). **(B)** Survival of mice injected with IL-22 or vehicle 1 hour after CLP surgery (n=9). **(C)** Lung sections were stained with H&E 12 hours after CLP, and the **(D)** lung injury score was calculated. Scale bar, 100 μ m. **(E)** Total number of cells in the BALF. **(F)** Total protein content in the BALF. **(G)** Wet/dry weight ratios of the mouse lung tissue. **(H)** Serum IL-1 β , IL-6 and TNF- α levels in the lung tissue. Significant differences were determined by a log-rank (Mantel-Cox) test (**A** and **B**) or one-way ANOVA with Bonferroni's multiple comparisons test (**D-I**). *P<0.05, **P<0.01, ***P<0.001.

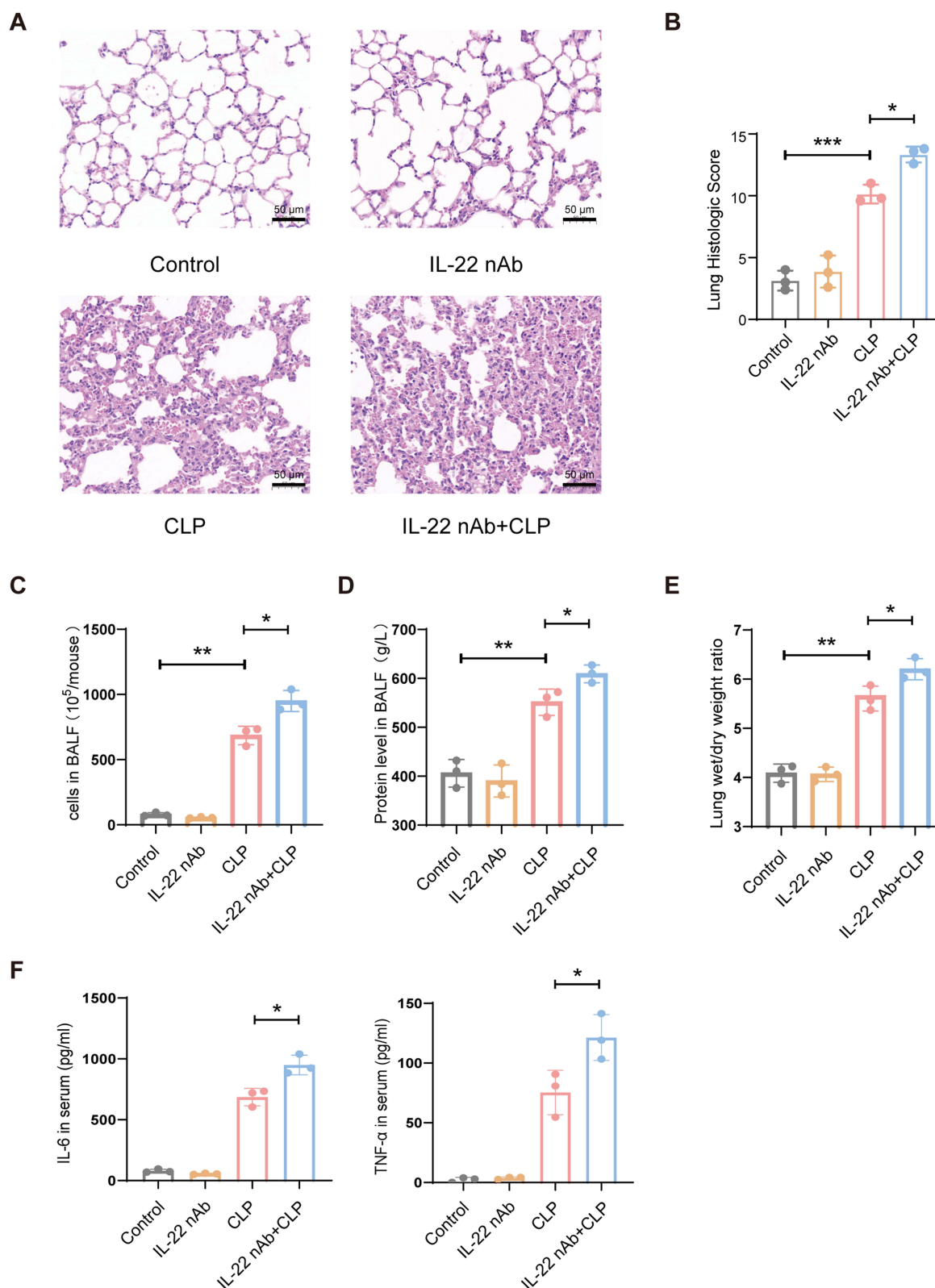


Figure 3 IL-22 nAb exacerbates SALI. The mice were intraperitoneally injected with an IL-22 nAb or an equivalent amount of isotype IgG before CLP surgery. **(A)** Lung sections were stained with H&E 12 hours after CLP, and the **(B)** lung injury score was calculated. **(C)** Total number of cells in BALF. Scale bar, 50 μ m. **(D)** Total protein content in the BALF. **(E)** Wet/dry weight ratios of mouse lungs. **(F)** Serum IL-6 and TNF- α levels. Significant differences were determined by one-way ANOVA with Bonferroni's multiple comparisons test (**B–F**). * $P < 0.05$, ** $P < 0.01$, *** $P < 0.001$.

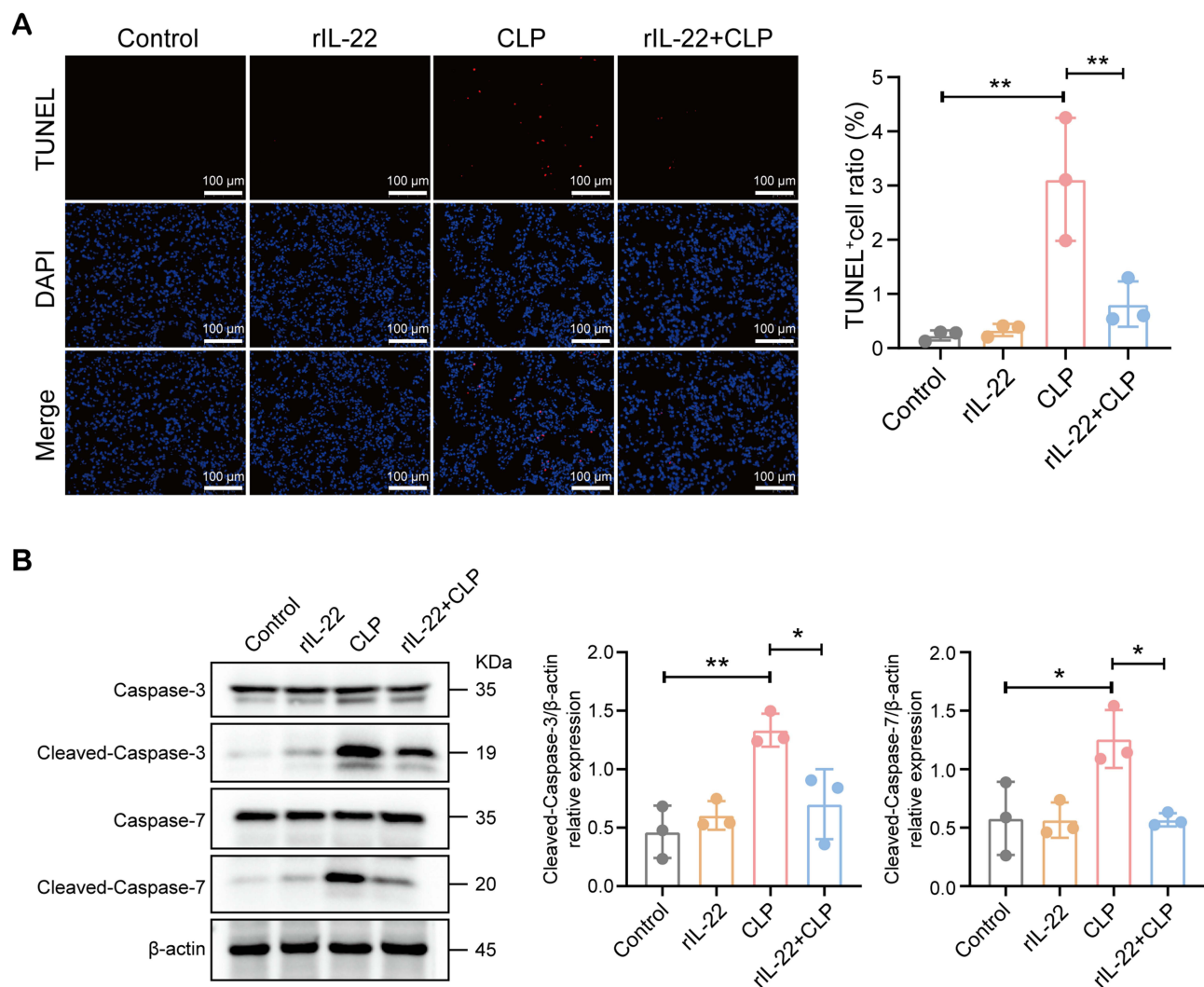


Figure 4 IL-22 inhibits apoptosis in the lung tissue of septic mice. The mice were pretreated with rIL-22 and the lung tissue was collected at 12 hours after CLP ($n=3$). **(A)** TUNEL assays revealed that IL-22 reversed the rate of apoptosis in the lungs of mice after CLP. Scale bar, 100 μ m. **(B)** Western blotting revealed that rIL-22 reversed the changes in the levels of cleaved caspase-3 and cleaved caspase-7 in septic mice. Significant differences were determined by one-way ANOVA with Bonferroni's multiple comparisons test (**A** and **B**). * $P<0.05$, ** $P<0.01$.

their cellular activity and promoted LDH release. Additionally, flow cytometry revealed a significant increase in early apoptosis after 24 hours of LPS (500 μ g/mL) stimulation (Figure 5C and D). Therefore, we used this concentration for subsequent cell experiments. As shown in Figure 6A, cell viability significantly decreased after LPS stimulation but gradually increased with rIL-22 treatment in a dose dependent manner. In addition, treatment with 50 ng/mL rIL-22 ameliorated the LPS-induced increase in LDH release (Figure 6B). These findings suggest that IL-22 treatment attenuates LPS-induced cellular damage. Moreover, flow cytometry revealed that the administration of IL-22 significantly inhibited the LPS-induced apoptosis of BEAS-2B cells (Figure 6C and D). We also performed an immunofluorescence analysis of cleaved caspase-3 and found that lung epithelial cells presented significantly increased green fluorescence after LPS stimulation. However, the intensity of green fluorescence significantly decreased after rIL-22 treatment (Figure 6E). Furthermore, we found that rIL-22 treatment mitigated the LPS-induced increase in the expression of cleaved caspase-3, while the expression of caspase-3 did not significantly increase, as shown by Western blotting (Figure 6F). These results indicate that IL-22 attenuates LPS-induced apoptosis and thus exerts protective effects.

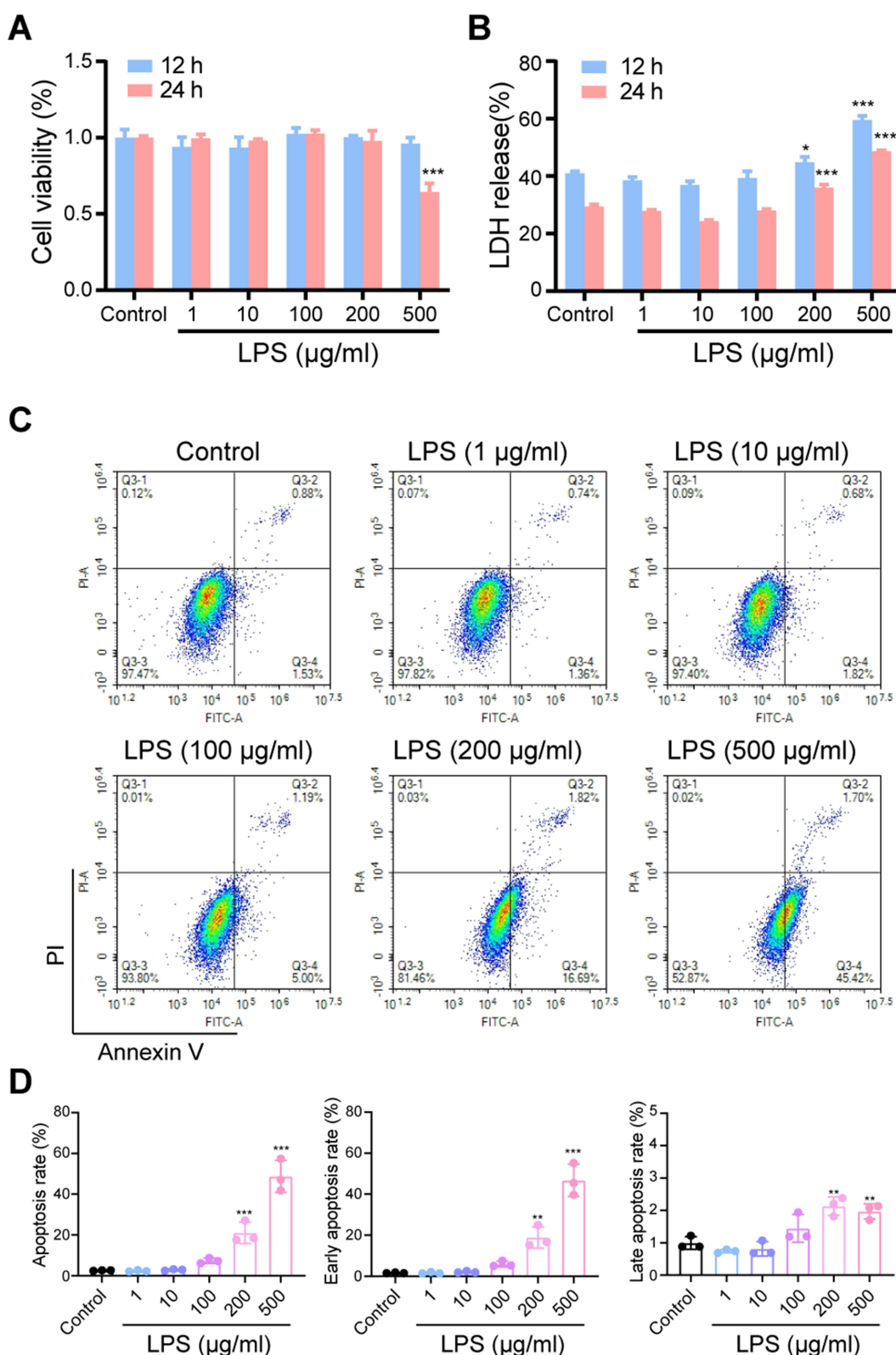


Figure 5 LPS promotes apoptosis in lung epithelial cells. **(A)** A CCK8 assay was used to examine the cytotoxicity of different concentrations of LPS at 12 hours and 24 hours. **(B)** Analysis of LDH levels in the cell culture medium after treatment with different concentrations of LPS for 12 hours and 24 hours. **(C)** BEAS-2B cells were stained with annexin V-FITC and propidium iodide (PI) and subjected to flow cytometry to examine the rates of apoptosis after treatment with different concentrations of LPS for 24 hours. **(D)** The percentages of early, late, and total apoptotic cells were quantified after LPS stimulation. All the samples were compared with the control. Significant differences were determined by one-way ANOVA with Bonferroni's multiple comparisons test (**A**, **B** and **D**). * $P < 0.05$, ** $P < 0.01$, *** $P < 0.001$.

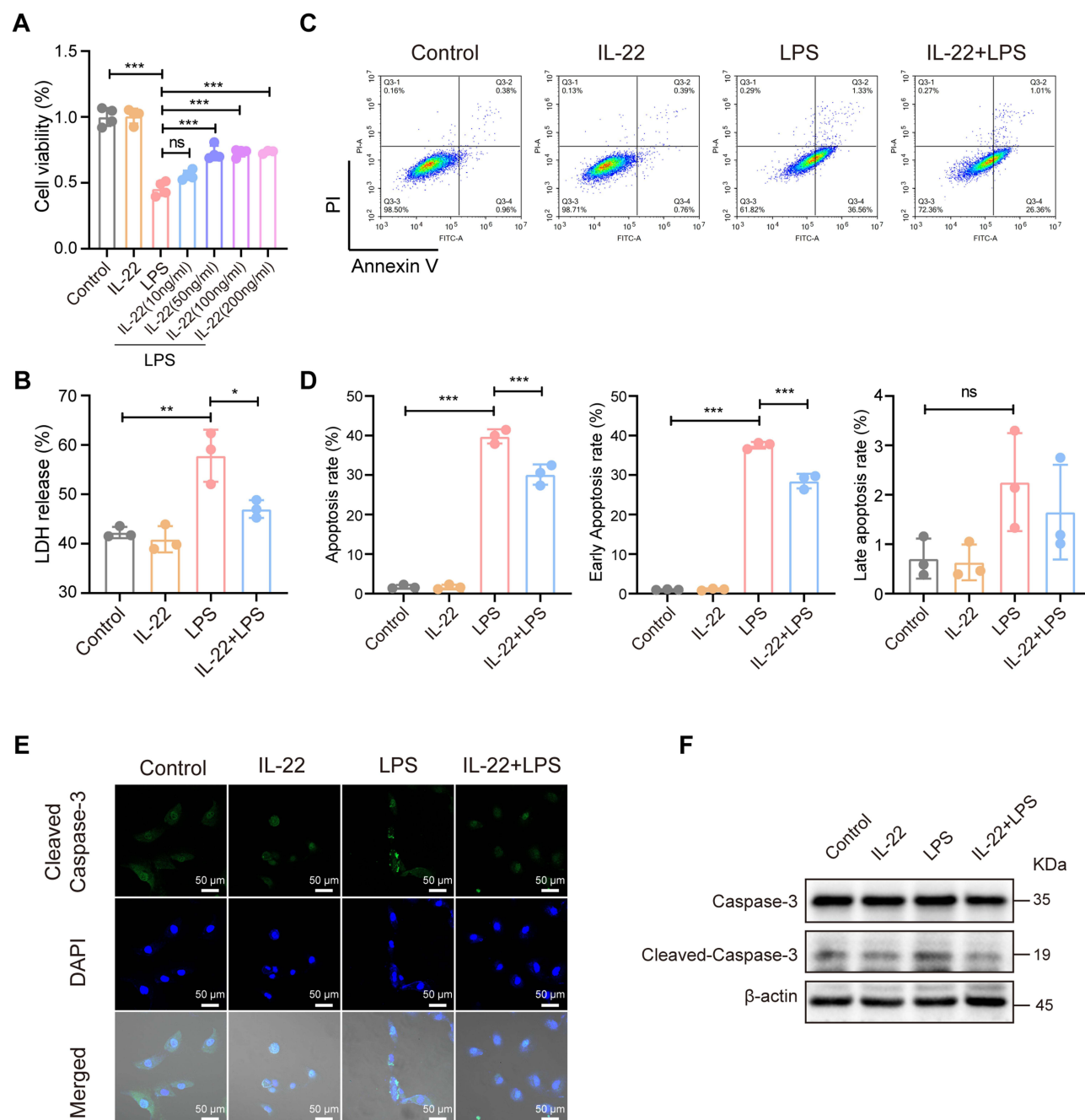


Figure 6 IL-22 attenuates LPS-induced apoptosis in BEAS-2B cells. **(A)** A CCK-8 assay was used to examine cytotoxicity in response to LPS stimulation with or without pretreatment with different concentrations of IL-22 for 24 hours. **(B)** Analysis of LDH release in response to LPS stimulation with or without IL-22 pretreatment for 24 hours. **(C)** BEAS-2B cells were stained with Annexin V-FITC and propidium iodide (PI) and subjected to flow cytometry to examine apoptosis in response to LPS stimulation with or without IL-22 pretreatment. **(D)** The percentages of early, late, and total apoptotic cells were quantified after LPS stimulation with or without IL-22 pretreatment. **(E)** The expression of cleaved caspase-3 in lung epithelial cells was examined via an immunofluorescence assay. Scale bar, 50 μm. **(F)** The expression of Caspase-3 and cleaved Caspase-3 in BEAS-2B cells in response to LPS stimulation and pretreatment with or without IL-22 for 24 hours was determined by Western blotting. Significant differences were determined by one-way ANOVA with Bonferroni's multiple comparisons test (**A**, **B** and **D**). *P<0.05, **P<0.01, ***P<0.001.

Abbreviation: ns, not significant (P>0.05).

rIL-22 Attenuated Apoptosis by Activating STAT3 in LPS-Stimulated BEAS-2B Cells

A previous study indicated that IL-22 attenuated liver injury by inhibiting apoptosis in a manner dependent on the activation of STAT3 signalling.²⁶ In this study, we elucidated whether IL-22 mediated the phosphorylation of STAT3 in LPS-stimulated lung epithelial cells. As shown in **Figure 7A**, the phosphorylation of STAT3 was notably elevated in the

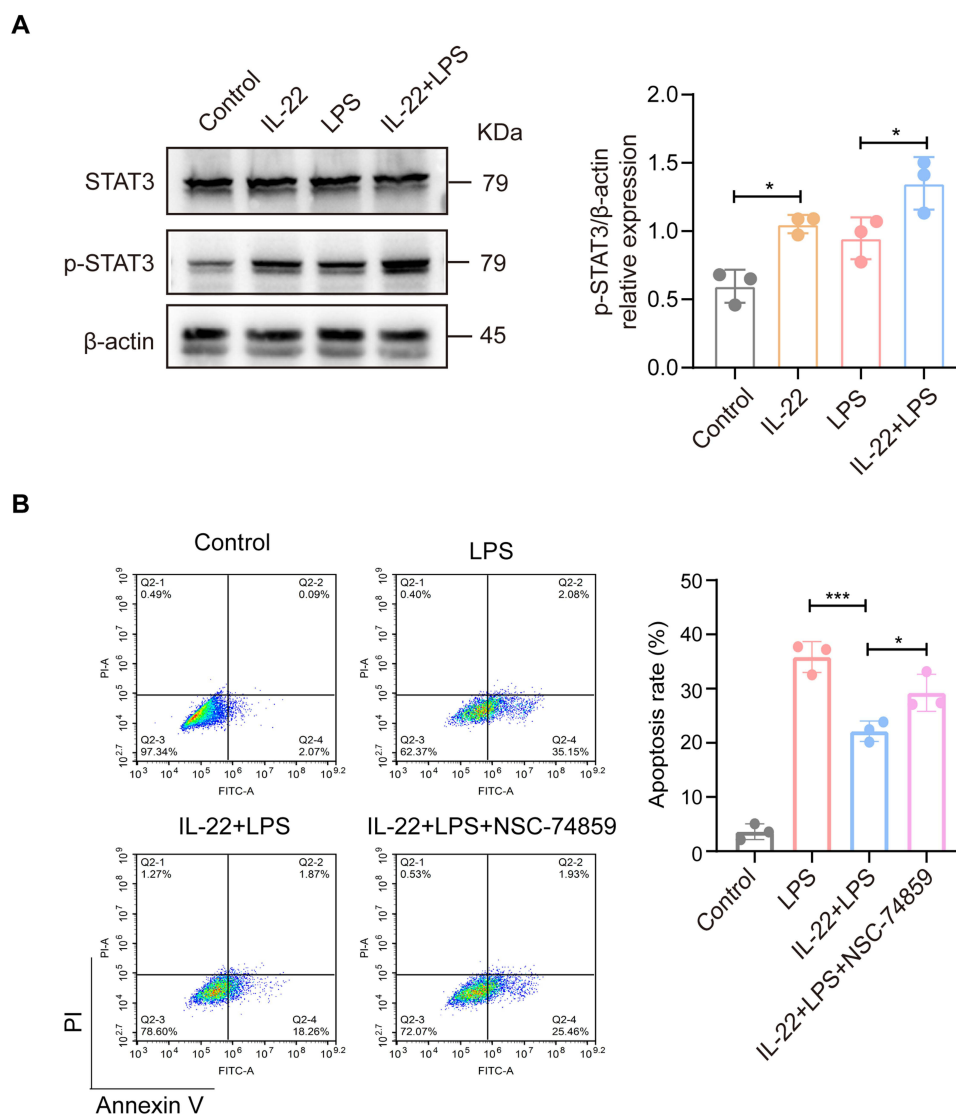


Figure 7 IL-22 inhibits apoptosis by activating STAT3 signalling in BEAS-2B cells. **(A)** Western blotting analysis of STAT3 and p-STAT3 expression in BEAS-2B cells with or without rIL-22 pretreatment and LPS stimulation. **(B)** BEAS-2B cells were stained with annexin V-FITC and propidium iodide (PI) and subjected to flow cytometry to examine the apoptosis rates in response to LPS stimulation with or without IL-22 pretreatment and a STAT3 inhibitor (50 μ M, NSC74859, MCE). The percentages of total apoptotic cells were quantified. Significant differences were determined by one-way ANOVA with Bonferroni's multiple comparisons test. * $P < 0.05$, *** $P < 0.001$.

group stimulated with IL-22 plus LPS. However, the expression of total STAT3 was not different between the two groups. STAT3 regulates cellular homeostasis through a complex regulatory network. Phosphorylation of STAT3 can play an anti-apoptotic role.²⁷ LPS stimulation of epithelial cells promotes STAT3 phosphorylation, and STAT3 phosphorylation may be a self-protective mechanism of the cell itself. Upon co-stimulation of cells with LPS and IL-22, the STAT3 signalling pathway was further activated, thereby amplifying the protective effect of STAT3 phosphorylation. Moreover, IL-22 treatment reduced the level of cleaved caspase-3, which was induced by LPS, and this effect was attenuated when BEAS-2B cells were pretreated with a STAT3 inhibitor (Figure 7B). These results suggest that the IL-22-mediated inhibition of LPS-induced apoptosis may occur through the activation of the STAT3 signalling pathway.

Discussion

During sepsis, overactivation of the immune system causes extensive inflammation that has the potential to cause tissue damage, organ failure and even death. Moreover, the specific immune response also assumes a vital function in mediating repair and tissue regeneration following injury.²⁸ This response leads to the recruitment of many types of immune cells.

IL-22, which was initially designated as an IL-10-related T-cell-derived inducible factor (IL-TIF), has attracted significant attention in recent years. IL-22 is synthesized primarily by immunocytes when the body is injured or infected.^{5–7} In this study, we discovered a marked increase in the serum IL-22 level in CLP mice compared with that in sham mice, and this increase corresponded to the severity of CLP (Figure 1A and B). IL-22 needs to bind to IL-22R, which is distributed on the outer membrane of epithelial cells, to exert its biological effects.^{29,30} In this study, we found that IL-22 was predominantly distributed in the bronchial epithelium of mice after CLP surgery (Figure 1C and D). Therefore, IL-22 may play an important role in bronchial epithelial cells during sepsis.

Recent research has demonstrated that IL-22 has multiple protective effects, including promoting regeneration, proliferation and repair during inflammatory diseases.^{15,31,32} Liu EH et al reported that IL-22 alleviated sepsis-induced acute liver injury, resulting in a reduction in liver cell apoptosis.³³ Shao L et al demonstrated that pretreatment with IL-22 induced autophagy in hepatocytes, thereby protecting against LPS-induced liver injury in mice.¹⁶ Yu C et al demonstrated that IL-22 played a protective role in endotoxemia by inducing the development of immunosuppressive cells.³⁴ In this study, we found that both pretreatment and posttreatment with rIL-22 increased the survival rate of CLP mice. We also found that rIL-22 treatment alleviated SALI, as evidenced by reduced histopathological changes and proinflammatory cytokine levels (Figure 2). Additionally, CLP-induced lung tissue damage and serum inflammatory cytokine secretion were significantly exacerbated after pretreatment with an IL-22 nAb (Figure 3). These results revealed that IL-22 played a protective role in a CLP-induced sepsis model.

However, several other studies have reached different conclusions. Weber GF et al demonstrated that inhibiting IL-22 with IL-22BP could increase the accumulation of immunocytes, reduce the bacterial load at the site of infection, enhance bacterial clearance and improve kidney injury in a colon ascendens stent peritonitis (CASP)-induced sepsis model, which caused a heavy systemic infection.²⁰ Yan Z et al reported that rIL-22 could increase the neutrophil count in the model of ALI that was induced by intratracheal injection of LPS.¹⁸ Both studies attempted to demonstrate that IL-22 played a destructive role in inflammatory diseases by affecting neutrophil aggregation. The differences between our study results and these previous findings may stem from differences in the models. Based on the biological complexity, the same protein may lead to different conclusions in different research models. In addition, the focus of this study was to embody the direct protective effect of IL-22 on epithelial cells, which are an important part of the lung barrier. When the body is exposed to pathogenic microorganisms or other stimuli, barrier cell integrity is important for removing harmful substances, limiting the development of infection, and maintaining homeostasis. Apoptosis of lung epithelial cells promotes the spread of lung inflammation and exacerbates the development of ALI. In this study, we found that the administration of rIL-22 ameliorated SALI in mice by decreasing lung apoptosis (Figure 4). However, pretreatment with an IL-22 nAb significantly increased the level of apoptosis in mouse lung tissues (Supplementary Figure 2). Our study also suggested that IL-22 mitigated the epithelial cell apoptosis induced by LPS *in vitro*, partially by inhibiting the expression of apoptosis-related proteins (Figure 6). These results indicate that IL-22 is associated with the inhibition of apoptosis during the development of sepsis.

Previous studies have demonstrated that IL-22 can bind to IL-22 receptors and subsequently activate or inhibit several signalling pathways, such as the STAT1/3/5, NF- κ B and MAPK pathways.^{9–11} The phosphorylation of STAT3, which can increase the transactivation of these signalling pathways, appears to serve as a significant mediator of IL-22 signalling.³⁵ Therefore, we examined the level of phosphorylated STAT3 via Western blotting. We detected a significant increase in STAT3 phosphorylation after IL-22 pretreatment of LPS-stimulated BEAS-2B cells (Figure 7A). Furthermore, STAT3 inhibitors significantly inhibited the antiapoptotic effect of IL-22 (Figure 7B). These findings highlight the importance of STAT3 as a critical factor in mediating the beneficial effects of IL-22 in mitigating septic conditions.

Several limitations of our study need to be considered. In this study, we used a mouse CLP model for *in vivo* experiments and LPS-stimulated BEAS-2B cells to mimic ALI in sepsis. Although both of these models have general applicability in the field of sepsis, they cannot fully simulate the specific pathogenesis of sepsis. In addition, when sepsis occurs in animal models, the specific cell types and regulatory factors of IL-22 are still unknown and require further study.

Conclusion

The present study demonstrated that the level of IL-22 was substantially increased in the serum and lung tissue of CLP mice. Administering rIL-22 before or after CLP led to an increased survival rate in mice with sepsis. Pretreatment with

rIL-22 alleviated SALI, whereas inhibition of the IL-22 pathway aggravated SALI. Our findings reveal that IL-22 protects against SALI, which has potential for advancing the development of new therapies for ALI.

Abbreviations

IL-22, interleukin-22; SALI, sepsis-induced acute lung injury; CLP, caecal ligation and puncture; LPS, lipopolysaccharide; rIL-22, recombinant IL-22; IL-22 nAb, IL-22 neutralizing antibody; STAT1/3/5, signal transducer and activator of transcription 1/3/5; ARDS, acute respiratory distress syndrome; BALF, bronchoalveolar lavage fluid; ELISA, enzyme-linked immunosorbent assay; TUNEL, terminal deoxynucleotidyl transferase-mediated nick-end labelling; LDH, lactate dehydrogenase.

Data Sharing Statement

The data that support the findings of this study are available from the corresponding author upon reasonable request.

Acknowledgments

This study was supported by the National Cancer Center/National Clinical Research Center for Cancer/Cancer Hospital & Shenzhen Hospital, Chinese Academy of Medical Sciences and Peking Union Medical College, Shenzhen (SZ2020ZD012), the Sanming Project of Medicine in Shenzhen (No. SZSM202311003) and the Dongguan Science and Technology of Social Development Program (20231800932402).

Disclosure

The authors report no conflicts of interest in this work. This paper has been uploaded as a preprint to the Research Square website: <https://www.researchsquare.com/article/rs-4198943/v1>.

References

1. Rehn M, Chew MS, Olkkola KT, Ingi Sigurðsson M, Yli-Hankala A, Hylander Møller M. Surviving sepsis campaign: international guidelines for management of sepsis and septic shock in adults 2021-endorsement by the Scandinavian society of anaesthesiology and intensive care medicine. *Acta Anaesthesiol Scand*. 2022;66(5):634–635. doi:10.1111/aas.14045
2. Gupta N, Matthay MA. Sepsis and stretch: synergistic effects on alveolar epithelial cell death? *Crit Care Med*. 2006;34(6):1846–1847. doi:10.1097/01.CCM.0000219378.52859.B1
3. Kumar V. Pulmonary innate immune response determines the outcome of inflammation during pneumonia and sepsis-associated acute lung injury. *Front Immunol*. 2020;11:1722. doi:10.3389/fimmu.2020.01722
4. Lam TY, Nguyen N, Peh HY, et al. ISM1 protects lung homeostasis via cell-surface GRP78-mediated alveolar macrophage apoptosis. *Proc Natl Acad Sci U S A*. 2022;119(4):e2019161119. doi:10.1073/pnas.2019161119
5. Rutz S, Noubade R, Eidenschenk C, et al. Transcription factor c-Maf mediates the TGF- β -dependent suppression of IL-22 production in TH17 cells. *Nat Immunol*. 2011;12(12):1238–1245. doi:10.1038/ni.2134
6. Yeste A, Mascanfroni ID, Nadeau M, et al. IL-21 induces IL-22 production in CD4⁺ T cells. *Nat Commun*. 2014;5(1):1–13.
7. Duhon T, Geiger R, Jarrossay D, Lanzavecchia A, Sallusto F. Production of interleukin 22 but not interleukin 17 by a subset of human skin-homing memory T cells. *Nat Immunol*. 2009;10(8):857–863. doi:10.1038/ni.1767
8. Hu H, Li L, Yu T, Li Y, Tang Y. Interleukin-22 receptor 1 upregulation and activation in hypoxic endothelial cells improves perfusion recovery in experimental peripheral arterial disease. *Biochem Biophys Res Commun*. 2018;505(1):60–66. doi:10.1016/j.bbrc.2018.08.163
9. Wolk K, Witte E, Witte K, Warszawska K, Sabat R. Biology of interleukin-22. *Semin Immunopathol*. 2010;32:17–31.
10. Jiang R, Sun B. IL-22 signaling in the tumor microenvironment. *Tumor Microenviron*. 2021:81–88.
11. Yu J, Xiao Z, Zhao R, Lu C, Zhang Y. Paeoniflorin suppressed IL-22 via p38 MAPK pathway and exerts anti-psoriatic effect. *Life Sci*. 2017;180:17–22. doi:10.1016/j.lfs.2017.04.019
12. Fang S, Ju D, Lin Y, Chen W. The role of interleukin-22 in lung health and its therapeutic potential for COVID-19. *Front Immunol*. 2022;13:951107.
13. Wu Z, Hu Z, Cai X, et al. Interleukin 22 attenuated angiotensin II induced acute lung injury through inhibiting the apoptosis of pulmonary microvascular endothelial cells. *Sci Rep*. 2017;7(1):2210. doi:10.1038/s41598-017-02056-w
14. Hoegl S, Bachmann M, Scheiermann P, et al. Protective properties of inhaled IL-22 in a model of ventilator-induced lung injury. *Am J Respir Cell Mol Biol*. 2011;44(3):369–376. doi:10.1165/rcmb.2009-0440OC
15. Sakamoto K, Kim Y-G, Hara H, et al. IL-22 controls iron-dependent nutritional immunity against systemic bacterial infections. *Sci Immunol*. 2017;2(8):eaai8371. doi:10.1126/sciimmunol.aai8371
16. Shao L, Xiong X, Zhang Y, et al. IL-22 ameliorates LPS-induced acute liver injury by autophagy activation through ATF4-ATG7 signaling. *Cell Death Dis*. 2020;11(11):970. doi:10.1038/s41419-020-03176-4
17. Pham TAN, Clare S, Goulding D, et al. Epithelial IL-22RA1-mediated fucosylation promotes intestinal colonization resistance to an opportunistic pathogen. *Cell Host Microbe*. 2014;16(4):504–516. doi:10.1016/j.chom.2014.08.017
18. Yan Z, Xiaoyu Z, Zhixin S, et al. Rapamycin attenuates acute lung injury induced by LPS through inhibition of Th17 cell proliferation in mice. *Sci Rep*. 2016;6(1):20156. doi:10.1038/srep20156

19. Whittington HA, Armstrong L, Uppington KM, Millar AB. Interleukin-22: a potential immunomodulatory molecule in the lung. *Am J Respir Cell mol Biol.* **2004**;31(2):220–226. doi:10.1165/rcmb.2003-0285OC
20. Weber GF, Schlautkötter S, Kaiser-Moore S, Altmayr F, Holzmann B, Weighardt H. Inhibition of interleukin-22 attenuates bacterial load and organ failure during acute polymicrobial sepsis. *Infect Immun.* **2007**;75(4):1690–1697. doi:10.1128/IAI.01564-06
21. Rittirsch D, Huber-Lang MS, Flierl MA, Ward PA. Immunodesign of experimental sepsis by cecal ligation and puncture. *Nat Protoc.* **2009**;4(1):31–36. doi:10.1038/nprot.2008.214
22. Busbee PB, Menzel L, Alrafas HR, et al. Indole-3-carbinol prevents colitis and associated microbial dysbiosis in an IL-22–dependent manner. *JCI Insight.* **2020**;5(1). doi:10.1172/jci.insight.127551
23. Fan Y, Chen J, Liu D, et al. HDL-S1P protects endothelial function and reduces lung injury during sepsis in vivo and in vitro. *Int J Biochem Cell Biol.* **2020**;126:105819. doi:10.1016/j.biocel.2020.105819
24. Beretta E, Romanò F, Sancini G, Grotberg JB, Nieman GF, Miseroocchi G. Pulmonary interstitial matrix and lung fluid balance from normal to the acutely injured lung. *Front Physiol.* **2021**;12:781874. doi:10.3389/fphys.2021.781874
25. Lakhani SA, Masud A, Kuida K, et al. Caspases 3 and 7: key mediators of mitochondrial events of apoptosis. *Science.* **2006**;311(5762):847–851. doi:10.1126/science.1115035
26. Jiang Z, Li W, Yu S, et al. IL-22 relieves hepatic ischemia-reperfusion injury by inhibiting mitochondrial apoptosis based on the activation of STAT3. *Int J Biochem Cell Biol.* **2024**;166:106503. doi:10.1016/j.biocel.2023.106503
27. Xing W-W, Zou M-J, Liu S, et al. Hepatoprotective effects of IL-22 on fulminant hepatic failure induced by d-galactosamine and lipopolysaccharide in mice. *Cytokine.* **2011**;56(2):174–179. doi:10.1016/j.cyto.2011.07.022
28. Oishi Y, Manabe I. Macrophages in inflammation, repair and regeneration. *Int Immunol.* **2018**;30(11):511–528. doi:10.1093/intimm/dxy054
29. Witte E, Witte K, Warsawska K, Sabat R, Wolk K. Interleukin-22: a cytokine produced by T, NK and NKT cell subsets, with importance in the innate immune defense and tissue protection. *Cytokine Growth Factor Rev.* **2010**;21(5):365–379. doi:10.1016/j.cytogfr.2010.08.002
30. Sonnenberg GF, Fouser LA, Artis D. Border patrol: regulation of immunity, inflammation and tissue homeostasis at barrier surfaces by IL-22. *Nat Immunol.* **2011**;12(5):383–390. doi:10.1038/ni.2025
31. Lindemans CA, Calafiore M, Mertelsmann AM, et al. Interleukin-22 promotes intestinal-stem-cell-mediated epithelial regeneration. *Nature.* **2015**;528(7583):560–564. doi:10.1038/nature16460
32. Zhuang L, Ma W, Yan J, Zhong H. Evaluation of the effects of IL-22 on the proliferation and differentiation of keratinocytes in vitro. *mol Med Rep.* **2020**;22(4):2715–2722. doi:10.3892/mmr.2020.11348
33. Liu E, Zheng Z, Xiao C, Liu X, Lin X. IL-22 relieves sepsis-induced liver injury via activating JAK/STAT3 signaling pathway. *J Biol Regul Homeost Agents.* **2020**;34(5):1719–1727. doi:10.23812/20-326-A
34. Yu C, Ling Q, Jiao J, et al. Interleukin-22 protects from endotoxemia by inducing suppressive F4/80+ Ly6G^{hi}Ly6C^{hi} cells population. *BMC Immunol.* **2022**;23(1):45. doi:10.1186/s12865-022-00511-6
35. Chiang H-Y, Lu -H-H, Sudhakar JN, et al. IL-22 initiates an IL-18-dependent epithelial response circuit to enforce intestinal host defence. *Nat Commun.* **2022**;13(1):874.

Journal of Inflammation Research

Publish your work in this journal

The Journal of Inflammation Research is an international, peer-reviewed open-access journal that welcomes laboratory and clinical findings on the molecular basis, cell biology and pharmacology of inflammation including original research, reviews, symposium reports, hypothesis formation and commentaries on: acute/chronic inflammation; mediators of inflammation; cellular processes; molecular mechanisms; pharmacology and novel anti-inflammatory drugs; clinical conditions involving inflammation. The manuscript management system is completely online and includes a very quick and fair peer-review system. Visit <http://www.dovepress.com/testimonials.php> to read real quotes from published authors.

Submit your manuscript here: <https://www.dovepress.com/journal-of-inflammation-research-journal>

Dovepress
Taylor & Francis Group